This is an Accepted Manuscript of an article published in [*Vet J.*], available online at http://www.sciencedirect.com/science/article/pii/S1090023314000744http://www.tandfonline.com/[Article DOI].

Please cite as:

Barrs, V. R., Beatty, J. A., Dhand, N. K., Talbot, J. J., Bell, E., Abraham, L. A., Chapman, P, Bennett, S, van Doorn, T., Makara, M. (2014). Computed tomographic features of feline sino-nasal and sino-orbital aspergillosis. *Vet J.* 201(2):215-22. DOI:10.1016/j.tvjl.2014.02.020

Computed tomographic features of feline sino-nasal and sino-orbital aspergillosis

V.R. Barrs [a,*], J.A. Beatty [a], N.K. Dhand [b], J.J. Talbot [a], E. Bell [c], L.A. Abraham [c], P. Chapman [d], S. Bennett [e], T. van Doorn [f], M. Makara [a]

[a] *Valentine Charlton Cat Centre, Faculty of Veterinary Science, The University of Sydney, Australia*

[b] *Farm Animal and Veterinary Public Health, Faculty of Veterinary Science, University of Sydney, New South Wales 2570, Australia*

[c] *University of Melbourne Veterinary Clinic and Hospital, Werribee, Victoria 3030, Australia*

[d] *Veterinary Speciality and Emergency Centre, Levittown, 301 Veterans Highway, Philadelphia 19056, USA*

[e] *Department of Veterinary Clinical Sciences, Murdoch University, Murdoch, Western Australia 6150, Australia*

[f] *Department of Applied and Industrial Mycology, CBS-KNAW Fungal Biodiversity Centre, Utrecht, Netherlands*

* Corresponding author. Tel.: +61 2 93513437.
E-mail address: vanessa.barrs@sydney.edu.au (V.R. Barrs).

Abstract

Feline upper respiratory tract aspergillosis (URTA) occurs as two distinct anatomic forms, sino-nasal aspergillosis (SNA) and sino-orbital aspergillosis (SOA). An emerging pathogen, *Aspergillus felis* is frequently involved. The pathogenesis of URTA, in particular, the relationship between the infecting isolate and outcome, is poorly understood. Computed tomography was used to investigate the route of fungal infection and extension in 16 cases (SNA *n*=7, SOA *n*=9) where the infecting isolate had been identified by molecular testing.

All cases had nasal cavity involvement except one cat with SNA that had unilateral frontal sinus changes. A strong association between the infecting species and anatomic form was identified. *A. fumigatus* infections remained within the sino-nasal cavity. Cryptic species infections were associated

with orbital and paranasal soft-tissue involvement and with orbital lysis. These species were further associated with a mass in the nasal cavity, paranasal sinuses or nasopharynx. Orbital masses showed heterogeneous contrast enhancement, with central coalescing hypoattenuating foci and peripheral rim enhancement. Severe, cavitated turbinate lysis, typical of canine SNA, was present only in cats with SNA.

These findings support that the nasal cavity is the portal of entry for fungal spores in feline URTA and that the route of extension to involve the orbit is via direct naso-orbital communication from bone lysis. Additionally, a pathogenic role for *A. wyomingensis* and a sinolith in a cat with *A. udagawae* infection are reported for the first time.

Keywords: Aspergillus felis; Aspergillosis; Cats; Sino-nasal; Sino-orbital

Introduction

Feline upper respiratory tract aspergillosis (URTA), first described in 1982, (Wilkinson et al., 1982), is being increasingly reported (Barachetti et al., 2009; Barrs et al., 2012; Declercq et al., 2012; Furrow and Groman, 2009; Giordano et al., 2010; Kano et al., 2008; Kano et al., 2013; Karnik et al., 2009; Smith and Hoffman, 2010). Disease occurs over a wide geographic range, including Australia, the USA, the United Kingdom, mainland Europe, and Japan (Barrs et al., 2012; Barrs et al., 2013; Declercq et al., 2012; Goodall et al., 1984; Kano et al., 2013; Smith and Hoffman, 2010; Tomsa et al., 2003). Two anatomic forms have been reported; sino-nasal aspergillosis (SNA) and sino-orbital aspergillosis (SOA) (Barrs et al., 2012). The environmental saprophytic fungi that cause these infections are most commonly from the *Aspergillus fumigatus* complex including *A. fumigatus* and *A. felis,* a closely related, recently discovered cryptic (*A. fumigatus*-mimetic) species (Barrs et al., 2012; Barrs et al., 2013; Kano et al., 2008; Kano et al., 2013; Whitney et al., 2013).

SNA and SOA have dramatically different prognoses (Barrs and Talbot, 2014). The determinants of these alternate outcomes are poorly understood. It is suspected that the nasal cavity (NC) is the route of infection in all cases and that SOA is an extension of NC infection, but systematic imaging studies to support this have not been carried out (Barrs et al., 2012). In humans with aspergillosis, invasion is generally associated with impaired host immunity rather than the virulence of the infecting fungal species (Romani, 2011). Data from feline cases suggest an influence of fungal species on pathogenesis; *A. fumigatus* infections are frequently associated with non-invasive sinonasal cavity (SNC) infections, while a cryptic species, A*. felis,* causes invasive sino-orbital disease (Barrs et al., 2012; Barrs et al., 2013).

Descriptions of computed tomography **(**CT) findings in cats with URTA are limited to case reports (Barachetti et al., 2009; Furrow and Groman, 2009; Giordano et al., 2010; Halenda and Reed, 1997; Hamilton et al., 2000; Kano et al., 2008; McLellan et al., 2006; Smith and Hoffman, 2010; Whitney et al., 2005), and one case series of mycotic rhinitis that included five cats with URTA but did not distinguish between SNA and SOA or identify the aetiological agents (Karnik et al., 2009). The objectives of this study were to describe the CT features of URTA, to determine whether cats with SOA have concurrent

involvement of the SNC, and to determine if there was any association between CT features and the form of aspergillosis and/or infecting species.

Materials and methods

CT examinations of the head of cats with confirmed URTA from February 2007 to October 2012 were identified retrospectively. Criteria for the diagnosis of URTA were identification of fungal hyphae on cytology or histology of tissue biopsies or sinonasal fungal plaques and molecular identification of the isolate using comparative sequence analyses of the internal transcribed spacer (ITS) regions (ITS1-5.8S-ITS2), partial β-tubulin and/or partial calmodulin genes (Barrs et al., 2013). Signalment data were collected for review.

CT examinations were included if thin bone and soft-tissue transverse images of the skull obtained perpendicular to the soft palate were available for review. CT examinations were performed at one of five centres (Table 1[1]; Phillips Brilliance, 16 Slice, Phillips Medical Systems; Toshiba Aquilion, 16-slice, Toshiba Medical Systems Corporation; Toshiba X vision, 1-slice helical, Toshiba Medical Systems Corporation; Siemens Somatom Duo, 2-slice helical scanner; Siemens Esprit plus, 1-slice helical scanner, Siemens AG, Medical Solutions). The field of view was adjusted to the individual skull dimensions and a 512 x 512 matrix was used.

CT scans were reviewed by a board certified radiologist (MM) blinded to isolate identity and clinical findings. Where more than one examination had been performed, the first was reviewed. Non-ionic iodinated contrast was administered at 660 mg/kg iodine IV (Omnipaque, GE Healthcare Ltd. Standard bone and soft-tissue window algorithms were used (Table 1). Images were reviewed using standardized bone (window width, 4500 HU; window level, 1100 HU) and soft-tissue (window width, 400 HU; window level, 40 HU) display settings.

Cases were assigned to one of two groups, SNA or SOA - based on absence or presence of a retrobulbar mass. Criteria for CT evaluation, adapted from a previous study (Karnik et al., 2009), included amount and laterality of soft-tissue attenuation within the SNC; extension of lesions within the NC; lysis and/or sclerosis of the bones forming the NC (turbinates, septum, nasal bone and adjacent maxilla) and paranasal bones (frontal bone, orbital bone (orbital lamina), palatine bone, zygomatic bone, tympanic bullae and cribriform plate); nasopharyngeal (NP) involvement, paranasal soft-tissue involvement and lymph-node involvement. Severity of NC lesions was graded as none, minimal (affecting less than one third), moderate (affecting two thirds) or severe (affecting more than two-thirds). The NC was divided into rostral (rostral to teeth 104 and 204), middle (extending from teeth 104 and 204 to 108 and 208) and caudal (caudal to teeth 108 and 208) regions. Lysis, soft-tissue attenuation and sclerosis of the paranasal bones were graded as none, minimal, moderate or severe. The pattern of contrast enhancement was described as none, normal mucosal enhancement, homogeneous, heterogeneous or peripheral.

[1] Tables and figures are presented at the end of this document.

Statistical analyses

Frequency tables were prepared for all variables. Associations between the two anatomic forms of URTA and aetiological agent (*A. fumigatus* vs cryptic species), and between anatomic form and variables indicative of soft-tissue attenuation, lysis and reactive bone lesions in nasal and paranasal regions were evaluated using contingency tables and Fisher's exact tests. Variables representing severity were collapsed into two categories–severe and non-severe–for statistical analyses because of limited number of observations in each class. A 5% level of significance was used and all *P*-values reported are two sided. Analyses were conducted using SAS software (2002–2003; SAS Institute).

Results

Sixteen cats met the inclusion criteria, including seven cats with SNA and nine cats with SOA. Post-contrast images were available in 13 cases (six SNA, seven SOA). One cat with SOA that had orbital exenteration before CT was excluded from statistical analyses of orbital CT features. Signalment data and molecular identity of fungal pathogens are presented (Table 2). Isolates not reported previously were *A. fumigatus* (two SNA; Cases 2 and 5), *A. felis* (two SOA; Cases 11 and 13), *A. udagawae* (two SOA; Cases 14 and 15) and *A. wyomingensis* (one SOA; Case 16). One cat with *A. fumigatus* infection was co-infected with *Scedosporium aurantiacum* (Case 5). Anatomic form was highly associated with infecting species; of cats with SNA five were infected with *A. fumigatus* and two with cryptic species, while all nine cats with SOA were infected with cryptic species (*P*=0.005) (Table 3). CT findings significantly associated with cryptic species infections included the presence of a mass in the NC, frontal sinus (FS), sphenoid sinus (SS) or NP; paranasal soft-tissue attenuation, orbital soft-tissue attenuation and orbital bone lysis (Table 3).

CT findings including frequency and severity of soft-tissue attenuation and bone lysis in the NC, nasopharynx, paranasal sinuses and tympanic bullae are presented in Table 4. All cats had NC involvement including increased soft-tissue attenuation and turbinate lysis, except one cat with SNA that had unilateral FS changes only. Of three cases with cryptic infections and focal soft-tissue NC masses, there was homogeneous enhancement in the two cases given contrast medium. Severe turbinate lysis occurred only in cats with SNA (three *A. fumigatus*, one *A. felis*) (*P*=0.005; Fig. 1). FS involvement was unilateral in 12 of 13 cases and was ipsilateral to the affected orbit in five cats with SOA. FS changes were characterised by soft tissue opacification without enhancement consistent with fluid or poorly vascularised tissue in 11 cases. FS attenuation was more severe in cats with SOA (*P*=0.040, Table 4). One case of SNA and *A. fumigatus* infection had moderate thickening of the FS mucosa with homogenous contrast enhancement, while another with SOA had a soft-tissue attenuating mass within the FS (Fig. 2). No contrast study was available for the latter. SS soft-tissue attenuation was accompanied by ipsilateral (*n*=8) or bilateral (*n*=1) FS involvement. SS changes were consistent with fluid in seven cases and with a mass in two cats with SOA. One showed central heterogeneous contrast enhancement and homogeneous peripheral enhancement. The other was a calcified density of 1835 HU, consistent with a sinolith, in a cat with *A. udagawae* infection (Fig. 3).

Of the 10 cats with increased soft-tissue attenuation of the nasopharynx (Table 4), five had homogeneous contrast enhancement of NP mucosa only, most consistent with fluid. Five other cats with

cryptic infections (four SOA; one SNA, *A. lentulus*) had a NP mass, with heterogeneous and homogeneous enhancement, respectively in the two cats with SOA in which contrast was administered.

Tympanic bullae changes were seen in two cases of SNA without NP involvement (Table 4). One showed minimal bullous effusion on the left side in the case with right FS involvement only. The other had bilateral NC involvement and a minimal soft-tissue attenuating mass in the bulla with homogenous contrast enhancement. Reactive bony changes of the nasal and paranasal bones are presented in Table 5. Nasal bone sclerosis was always accompanied by sclerosis of the frontal or zygomatic bone.

Paranasal bone lysis and soft-tissue abnormalities are described in Table 6. Cryptic species infections (n=11) were associated with orbital (P=0.002) or paranasal soft-tissue involvement (P=0.001) (Table 3). Orbital masses were characterised by heterogeneous contrast enhancement, with central coalescing hypoattenuating foci and peripheral rim enhancement (Fig. 6). Masses were located in the rostral and ventromedial aspect of the orbit causing dorsolateral displacement of the globe. The largest mass displaced the zygomatic arch laterally. Orbital masses typically extended rostrally to the rostral aspect of the zygomatic arch and caudally to the rostral aspect of the ramus of the mandible, immediately rostral to the temporomandibular joint. In all cases of SOA lateral extension into the paranasal maxillary soft-tissues was identified, resulting in a distinct mass effect in eight cases. Orbital masses extended ventrally into pterygopalatine fossa of the oral cavity in six cases (Fig. 4). Soft-tissue attenuation adjacent an area of complete lysis of the nasal bone was present in one cat with SNA and *A. felis* infection.

Orbital bone lysis was detected in both anatomic forms and was significantly associated with aetiological agent (Table 3 & 4). Orbital lysis was complete in four cases (two SNA, two SOA) and punctate in eight (two SNA, six SOA; Fig. 5). Of the four cats with frontal bone lysis two with SNA also had palatine bone lysis (Table 5). Frontal, palatine and zygomatic bone lysis was punctate in all cases except one cat with SOA and a focal area of severe complete palatine lysis. Severe mandibular lymph node enlargement was documented only in cases of SOA (P= 0.011). All enlarged lymph nodes enhanced homogeneously.

Discussion

This study of CT findings in feline sino-nasal and sino-orbital aspergillosis documented involvement of the SNC in all cases, regardless of the anatomic form. This supports the hypothesis that orbital involvement in feline SOA occurs subsequent to NC infection following inhalation of *Aspergillus* conidia, but evaluation of serial CTs over time would be required to definitively demonstrate extension of disease from the NC to the orbit. Upper respiratory tract signs can be absent at the time of diagnosis when exophthalmos is present (Barrs et al., 2012; Smith and Hoffman, 2010), but the extent of SNC involvement should be evaluated as this might inform therapeutic decisions. All cats with SOA had evidence of naso-orbital communication due to lysis of the orbital lamina, identifying direct extension as the likely route of orbital involvement. This is supported by findings on CT, surgery or at post-mortem in other cases, and by the fact that haematogenous spread has not been reported (Barachetti et al., 2009;

Barrs et al., 2012; Giordano et al., 2010; Hamilton et al., 2000; Wilkinson et al., 1982). Orbital extension directly from the frontal sinus has been documented in one case (Halenda and Reed, 1997).

Interestingly, orbital bone lysis was common regardless of anatomical form. In dogs with SNA due to *A. fumigatus*, orbital lysis is common whereas SOA is rare (Saunders et al., 2002). Thus, risk factors additional to orbital lysis are clearly necessary for the establishment of mycotic orbital disease in cats. Previous studies have found that *A. fumigatus* infections were confined to the SNC, while cases of SOA were caused by cryptic species, particularly *A. felis* (Barrs et al., 2013; Barrs and Talbot, 2014; Declercq et al., 2012; Kano et al., 2008; Kano et al., 2013). Imaging findings presented here are consistent with this putative role for fungal species in disease outcome. Species-specific fungal virulence factors could be involved in the establishment of invasive orbital disease. SOA in cats is similar to chronic granulomatous fungal rhinosinusitis of immunocompetent humans, an uncommon disease, reported in Africa and Asia and caused by *A. flavus,* which has a propensity to colonise the nasal and paranasal sinuses in hot, dry climates (Thompson and Patterson, 2012). Similar to humans and dogs with SNA, nasal and paranasal bone lysis in feline URTA is likely due to the host's pro-inflammatory response and fungal virulence factors such as dermonecrolytic toxins (Peeters and Clercx, 2007; Thompson and Patterson, 2012). Fungal osteomyelitis has not been reported in feline URTA.

In addition to SNC involvement, CT features common to both anatomic forms included unilateral involvement of paranasal sinuses, and paranasal bone lysis and/or sclerosis. Cribriform plate lysis, a relative contraindication for topical antifungal treatment in canine SNA (Day, 2009), was detected in 25% of cases highlighting the importance of CT evaluation in treatment planning. Some CT features were associated with infecting species and/or anatomic form. Orbital masses, abnormal paranasal soft-tissue attenuation and a mass effect in the NC, FS, SS or NP were only associated with cryptic species while severe "cavitated" lysis was only present in cats with SNA including three with *A. fumigatus* infection. In dogs *A. fumigatus* is the aetiological agent of SNA in 98% of cases (Talbot et al., 2014) and characteristic CT features include cavitated turbinate lysis, a rim of soft-tissue of variable thickness along bones in the FS, maxillary recess and nasal passages, abnormal presence of soft-tissue accumulation and reactive bony-change (Saunders et al., 2004; Saunders and Van Bree, 2003; Saunders et al., 2002). The finding of isolated FS involvement in one cat has been reported in canine SNA (Johnson et al., 2006).

Post-contrast features of orbital masses are similar to those reported in SOA in people and in mycotic rhinosinusitis due to non-*Aspergillus* spp, including cryptococcosis, in cats, (Karnik et al., 2009; Pushker et al., 2011; Sivak-Callcott et al., 2004). Central hypoattenuating foci have been interpreted as areas of necrosis and peripheral enhancement as inflammatory response (Almutairi et al., 2009; DeLone et al., 1999). A similar pattern of enhancement can be seen with neoplasia in humans, where peripheral enhancement has been interpreted as well-perfused, viable tumour tissue (Nino-Murcia et al., 2000). Whether post-contrast features will aid in differentiating SOA from neoplasia in cats requires characterisation of the latter.

Previous retrospective analysis of CT findings in feline sinonasal disease included few cases of mycotic rhinosinusitis (0—5%) (Schoenborn et al., 2003; Tromblee et al., 2006). CT features associated

with sinonasal neoplasia included lysis of the paranasal bones especially bilateral orbital bone lysis, moderate to severe turbinate destruction, lysis of the nasal septum, homogeneous mass within the sinonasal cavity, unilateral abnormal soft-tissue or fluid within the frontal or sphenoid sinuses and extension of the disease process into the orbit or paranasal facial soft-tissues (Schoenborn et al., 2003; Tromblee et al., 2006), were all features of aspergillosis in the current study.

Tympanic bulla changes were rare and likely incidental. In contrast, 28% of cats with sinonasal neoplasia or inflammatory disease were reported previously to have bulla effusion secondary to auditory tube obstruction or ascending infection. However, only one of the 46 cats in that study had a fungal aetiology (Detweiler et al., 2006).

Here we report sinolithiasis for the first time in feline URTA. Rhinolithiasis was reported in one cat previously with SNA (Tomsa et al., 2003). Sinoliths, described in 50-75% of humans with maxillary sinus fungal mycetomas, are deposits of calcium-containing fungal metabolites in necrotic areas of mycelial plaques. Predisposing factors include chronic inflammation, impaired sinus drainage and the presence of a nidus of material of endogenous or exogenous origin e.g. endodontic filling materials, around which calcification occurs (Lenglinger et al., 1996).

Molecular identification revealed two new isolates of *A. udagawae* from Australia and the USA. These, in addition to two previous isolates reported in Japan establish *A. udagawae* as the second most common cause of feline SOA (Kano et al., 2008; Kano et al., 2013). *A. udagawae* is the most common cryptic species to cause invasive pulmonary aspergillosis in humans (Vinh et al., 2009). *A. wyomingensis*, reported here for the first time as a cause of feline SOA and as a host pathogen, is a recently described soil saprophyte related to *A. felis* and to *A. udagawae* (Novakova et al., 2013). Accurate species identification is important, since cryptic species are more resistant to antifungal drugs than *A. fumigatus* (Barrs et al., 2013). Previous studies of feline URTA have identified that breeds of cats with brachycephalic conformation are over-represented (Barrs et al., 2012; Tomsa et al., 2003; Whitney et al., 2005). These have included Himalayans, Persians, Exotic shorthairs, American shorthairs and Ragdoll cats. Here we additionally report disease in British and Scottish shorthair cats. Prospective studies are required to determine whether the increased risk of URTA in these breeds of cats is genetic due to common ancestry, or if it is associated with SNC conformation combined with other factors such as viral upper respiratory tract infection (Barrs and Talbot, 2014).

The limitations of this study included the small sample size and its retrospective design, which precluded standardisation of CT conditions for each examination.

Conclusion

Common CT features of both anatomic forms of feline upper respiratory tract aspergillosis include asymmetric, bilateral sino-nasal cavity involvement, moderate to severe soft-tissue attenuation of the nasal cavity, sphenoid sinus and frontal sinus, moderate to severe turbinate lysis, and orbital bone lysis. A strong association was identified between the infecting fungal species and the anatomic form of disease. Cryptic species were significantly associated with sino-orbital aspergillosis, with the presence of

a mass in the nasal cavity, sinuses or nasopharynx, with paranasal soft-tissue attenuation, and with orbital bone lysis.

Conflict of interest statement

None of the authors has any financial or personal relationships that could inappropriately influence or bias the content of the paper.

Acknowledgements

The authors would like to thank Mrs Kathy Hughes and Mrs Helen Laurendet for technical assistance. Some data have been presented previously (Barrs et al., 2012, 2013).

References

Almutairi, B.M., Nguyen, T.B., Jansen, G.H., Asseri, A.H., 2009. Best Cases from the AFIP Invasive Aspergillosis of the Brain: Radiologic-Pathologic Correlation. Radiographics 29, 375-379.

Barachetti, L., Mortellaro, C.M., Di Giancamillo, M., Giudice, C., Martino, P., Travetti, O., Miller, P.E., 2009. Bilateral orbital and nasal aspergillosis in a cat. Veterinary Ophthalmology 12, 176-182.

Barrs, V., Halliday, C., Martin, P., Wilson, B., Krockenberger, M., Gunew, M., Bennett, S., Koehlmeyer, E., Thompson, A., Fliegner, R., Hocking, A., Sleiman, S., O'Brien, C., Beatty, J., 2012. Sinonasal and sino-orbital aspergillosis in 23 cats: aetiology, clinicopathological features and treatment outcomes. The Veterinary Journal 191, 58-64.

Barrs, V.R., Talbot, J., 2014. Feline Aspergillosis. Veterinary Clinics of North America, Small Animal Practice 44, 51-73.

Barrs, V.R., van Doorn, T., Houbraken, J., Kidd, S.E., Martin, P., Pinheiro, M.D., Richardson, M., Varga, J., Samson, R.A., 2013. Aspergillus felis sp. nov., an emerging agent of invasive aspergillosis in humans, cats and dogs. PLOS one 8, e64781.

Day, M.J., 2009. Canine sino-nasal aspergillosis: parallels with human disease. Medical Mycology 47, S315-S323.

Declercq, J., Declercq, L., Fincioen, S., 2012. Unilateral sino-orbital and subcutaneous aspergillosis in a cat. Vlaams Diergeneeskundig Tijdschrift 81, 357-362.

DeLone, D.R., Goldstein, R.A., Petermann, G., Salamat, M.S., Miles, J.M., Knechtle, S.J., Brown, W.D., 1999. Disseminated aspergillosis involving the brain - distribution and imaging characteristics. American Journal of Neuroradiology 20, 1597-1604.

Detweiler, D.A., Johnson, L.R., Kass, P.H., Wisner, E.R., 2006. Computed tomographic evidence of bulla effusion in cats with sinonasal disease: 2001-2004. Journal of Veterinary Internal Medicine 20, 1080-1084.

Furrow, E., Groman, R.P., 2009. Intranasal infusion of clotrimazole for the treatment of nasal aspergillosis in two cats. Javma-Journal of the American Veterinary Medical Association 235, 1188-1193.

Giordano, C., Gianella, P., Bo, S., Vercelli, A., Giudice, C., Della Santa, D., Tortorano, A.M., Peruccio, C., Peano, A., 2010. Invasive mould infections of the naso-orbital region of cats: a case involving *Aspergillus fumigatus* and an aetiological review. Journal of Feline Medicine and Surgery 12, 714-723.

Goodall, S.A., Lane, J.G., Warnock, D.W., 1984. The diagnosis and treatment of a case of nasal aspergillosis in a cat. . Journal of Small Animal Practice 25, 627-633.

Halenda, R.M., Reed, A.L., 1997. Ultrasound computed tomography diagnosis - Fungal, sinusitis and retrobulbar myofascitis in a cat. Veterinary Radiology and Ultrasound 38, 208-210.

Hamilton, H.L., Whitley, R.D., McLaughlin, S.A., 2000. Exophthalmos secondary to aspergillosis in a cat. Journal of the American Animal Hospital Association 36, 343-347.

Johnson, L.R., Drazenovich, T.L., Herrera, M.A., Wisner, E.R., 2006. Results of rhinoscopy alone or in conjunction with sinuscopy in dogs with aspergillosis: 46 cases (2001-2004). Javma-Journal of the American Veterinary Medical Association 228, 738-742.

Kano, R., Itamoto, K., Okuda, M., Inokuma, H., Hasegawa, A., Balajee, S.A., 2008. Isolation of *Aspergillus udagawae* from a fatal case of feline orbital aspergillosis. Mycoses 51, 360-361.

Kano, R., Shibahashi, A., Fujino, Y., Sakai, H., Mori, T., Tsujimoto, H., Yanai, T., Hasegawa, A., 2013. Two cases of feline orbital aspergillosis due to *A. udagawae* and *A. virdinutans*. Journal of Veterinary Medical Science 75, 7-10.

Karnik, K., Reichle, J.K., Fischetti, A.J., Goggin, J.M., 2009. Computed tomographic findings of fungal rhinitis and sinusitis in cats. Veterinary Radiology and Ultrasound 50, 65-68.

Lenglinger, F.X., Krennmair, G., MullerSchelken, H., Artmann, W., 1996. Radiodense concretions in maxillary sinus aspergillosis: Pathogenesis and the role of CT densitometry. European Radiology 6, 375-379.

McLellan, G.J., Aquino, S.M., Mason, D.R., Kinyon, J.M., Myers, R.K., 2006. Use of posaconazole in the management of invasive orbital aspergillosis in a cat. Journal of the American Animal Hospital Association 42, 302-307.

Nino-Murcia, M., Olcott, E.W., Jeffrey, R.B., Lamm, R.L., Beaulieu, C.F., Jain, K.A., 2000. Focal liver lesions: Pattern-based classification scheme for enhancement at arterial phase CT. Radiology 215, 746-751.

Novakova, A., Hubka, V., Dudova, Z., Matsuzawa, T., Kubatova, A., Yaguchi, T., Kolarik, M., 2013. New species in *Aspergillus* section *Fumigati* from relcamation sites in Wyoming (U.S.A.) and revision of *A. viridinutans* complex. Fungal Diverstiy. doi 10.1007/s13225-013-0262-5

Peeters, D., Clercx, C., 2007. Update on canine sinonasal aspergillosis. Veterinary Clinics of North America-Small Animal Practice 37, 901-916.

Pushker, N., Meel, R., Kashyap, S., Bajaj, M.S., Sen, S., 2011. Invasive aspergillosis of orbit in immunocompetent patients: treatment and outcome. Ophthalmology 118, 1886-1891.

Romani, L., 2011. Immunity to fungal infections. Nature Reviews Immunology 11, 275-288.

Saunders, J.H., Clercx, C., Snaps, F.R., Sullivan, M., Duchateau, L., van Bree, H.J., Dondelinger, R.E., 2004. Radiographic, magnetic resonance imaging, computed tomographic, and rhinoscopic features of nasal aspergillosis in dogs. Journal of the American Veterinary Medical Association 225, 1703-1712.

Saunders, J.H., Van Bree, H., 2003. Comparison of radiography and computed tomography for the diagnosis of canine nasal aspergillosis. Veterinary Radiology and Ultrasound 44, 414-419.

Saunders, J.H., Zonderland, J.L., Clercx, C., Gielen, I., Snaps, F.R., Sullivan, M., vanBree, H., Dondelinger, R.F., 2002. Computed tomographic findings in 35 dogs with nasal aspergillosis. Veterinary Radiology and Ultrasound 43, 5-9.

Schoenborn, W.C., Wisner, E.R., Kass, P.P., Dale, M., 2003. Retrospective assessment of computed tomographic imaging of feline sinonasal disease in 62 cats. Veterinary Radiology and Ultrasound 44, 185-195.

Sivak-Callcott, J.A., Livesley, N., Nugent, R.A., Rasmussen, S.L., Saeed, P., Rootman, J., 2004. Localised invasive sino-orbital aspergillosis: characteristic features. British Journal of Ophthalmology 88, 681-687.

Smith, L.N., Hoffman, S.B., 2010. A case series of unilateral orbital aspergillosis in three cats and treatment with voriconazole. Veterinary Ophthalmology 13, 190-203.

Talbot, J.J, Martin, P., Johnson, L., Sutton, D., Halliday, C., Beatty, J., Steiner, J., Gibson, J.S., Kidd, S.E., Barrs, V.R., 2014. What causes sino-nasal aspergillosis in dogs? A molecular approach to species identification. The Veterinary Journal, *In press,* Available online 23 January 2014.

Thompson, G.R., Patterson, T.F., 2012. Fungal disease of the nose and paranasal sinuses. Journal of Allergy and Clinical Immunology 129, 321-326.

Tomsa, K., Glaus, T.A., Zimmer, C., Greene, C.E., 2003. Fungal rhinitis and sinusitis in three cats. Journal of the American Veterinary Medical Association 222, 1380-1384.

Tromblee, T.C., Jones, J.C., Etue, A.E., Forrester, S.D., 2006. Association between clinical characteristics, computed tomography characteristics, and histologic diagnosis for cats with sinonasal disease. Veterinary Radiology and Ultrasound 47, 241-248.

Vinh, D.C., Shea, Y.R., Sugui, J.A., Parrilla-Castellar, E.R., Freeman, A.F., Campbell, J.W., Pittaluga, S., Jones, P.A., Zelazny, A., Kleiner, D., Kwon-Chung, K.J., Holland, S.M., 2009. Invasive aspergillosis due to *Neosartorya udagawae*. Clinical Infectious Diseases 49, 102-111.

Whitney, B.L., Broussard, J., Stefanacci, J.D., 2005. Four cats with fungal rhinitis. Journal of Feline Medicine and Surgery 7, 53-58.

Whitney, J., Beatty, J.A., Dhand, N., Briscoe, K., Barrs, V.R., 2013. Evaluation of serum galactomannan detection for the diagnosis of feline upper respiratory tract aspergillosis. Veterinary Microbiology 162, 180-185.

Wilkinson, G.T., Sutton, R.H., Grono, L.R., 1982. Aspergillus spp infection associated with orbital cellulitis and sinusitis in a cat. . Journal of Small Animal Practice 23, 127-131.

Table 1

Factors used for acquisition of computed tomographic images

Centre [a]	No. of cases	Reconstructed slice thickness bone tissue algorithm (mm)	Reconstructed slice thickness soft tissue algorithm (mm)	Beam collimation (No. of data channels)	Detector row width (mm)	Tube potential (kV)	Tube Current (mA)	Pitch Factor
VCCC	8	1	3	16	0.75	120	200	0.4
RPAH	2	0.75	3	16	0.75	120	200	0.4
UMVCH	3	2	2	1	0.75	120	100	1
MUVH	2	2	2	2	0.75	130	120	1
VSEC	1	1	1	1	1	130	60	1

[a] VCCC, Valentine Charlton Cat Centre, Sydney, Australia; RPAH, Royal Prince Alfred Hospital, Sydney, Australia; UMVTH, University of Melbourne Veterinary Clinic and Hospital, Melbourne, Australia; MUVH, Murdoch Veterinary Hospital, Perth, Australia; VSEC, Veterinary Specialist and Emergency Centre, Levittown, Philadelphia, USA.

Table 2

Signalment, aetiological agent and anatomic form of aspergillosis

Case	Age (years)	Sex [a]	Breed [a]	Form [a]	Species	Genbank accession nos.		
						ITS[a]	*benA*[a]	*CalM*[a]
1*	6.8	F	Ragdoll	SNA	*A. fumigatus*	-	-	-
2	8	F	SSH	SNA	*A. fumigatus*	-	-	-
3*	11	F	Persian	SNA	*A. fumigatus*	-	-	JX021722
4*	7.4	M	Persian	SNA	*A. fumigatus*	-	-	-
5	2.8	F	DSH	SNA	*A. fumigatus/ Scedosporium aurantiacum*	-	-	-
6*	14.8	F	DLH	SNA	*A. lentulus*	-	-	JX021720
7*	13	M	DLH	SNA	*A. felis*	JX021681	JX021704	JX021724
8*	5	F	CR	SOA	*A. felis*	JX021675	JX021694	JX021717
9*	2	M	HIM	SOA	*A. felis*	JX021682	JX021705	JX021725
10*	2	F	DSH	SOA	*A. felis*	JX021683	JX021706	JX021726
11	2.3	F	DSH	SOA	*A. felis*	-	-	-

12*	3.6	M	DSH	SOA	*A. felis*	KF558318	JX021700	JX021715
13	2.8	M	BSH	SOA	*A. felis*	KF703495	KF703496	-
14	4.1	M	Persian	SOA	*A. udagawae*	-	KF073497	KF703498
15	4.7	M	DSH	SOA	*A. udagawae*	-	KF703499	-
16	1.5	M	BSH	SOA	*A. wyomingensis*	JX021685	JX021709	-

[a] F, female (neutered); M, male (neutered); SSH, Scottish Shorthair; DSH, Domestic Shorthair; DLH, Domestic Longhair; CR, Cornish Rex; HIM, Himalayan; BSH, British Shorthair; SNA, sino-nasal aspergillosis; SOA, sino-orbital aspergillosis; ITS, internal transcribed spacer; *benA*, betatubulin; *CalM*, calmodulin

* Signalment and molecular identification reported previously (Barrs et al., 2012a; Barrs et al., 2013)

Table 3

Associations between aetiologic agent and anatomic form or computed tomographic features in cats with URTA

	Categories	*A. fumigatus* Frequency (%)	Cryptic species Frequency (%)	*P*-value
Anatomic form	SNA[a]	5 (71)	2 (29)	0.005
	SOA[a]	0 (0)	9 (100)	
NC, FS, SS or NP mass[b]	Yes	0 (0)	8 (100)	0.026
	No	5 (63)	3 (37)	
Paranasal soft-tissue involvement	Yes	0 (0)	10 (100)	0.001
	No	5 (83)	1 (17)	
Orbital soft-tissue involvement	Yes	0 (0)	9 (100)	0.002
	No	5 (83)	1 (17)	
Orbital bone lysis	Yes	2 (17)	10 (83)	0.022
	No	3 (100)	0 (0)	

[a] SNA, sino-nasal aspergillosis; SOA, sino-orbital aspergillosis

[b] NC, nasal cavity; FS, frontal sinus; SS, sphenoid sinus; NP, nasopharyngeal

Table 4

Soft-tissue attenuation and bone lysis in the nasal cavity, nasopharynx, paranasal sinuses and tympanic bullae on computed tomography in 16 cats with upper respiratory tract aspergillosis

	Categories	SNA Frequency (%)	SOA Frequency (%)	Total	*P*-value[a]
Type of sinonasal disease	Bilateral	5 (38)	8 (62)	13	0.55
	Unilateral	2 (67)	1 (33)	3	
Type of bilateral involvement	Asymmetrical	4 (36)	7 (64)	11	1.0
	Symmetrical	1 (50)	1 (50)	2	
Nasal region involved	Rostral to caudal	4 (44)	5 (56)	9	1
	Middle	1 (33)	2 (67)	3	
	Middle to caudal	1 (33)	2 (67)	3	
	Caudal	1 (100)	0 (0)	1	
Nasal cavity soft tissue attenuation	None	1 (100)	0 (0)	1	0.162
	Minimal	1 (33)	2 (67)	3	
	Moderate	3 (60)	2 (40)	5	
	Severe	2 (29)	5 (71)	7	
Turbinate lysis	None	1 (100)	0 (0)	1	0.005
	Minimal	2 (33)	4 (67)	6	
	Moderate	0 (0)	5 (100)	5	
	Severe	4 (100)	0 (0)	4	
Nasal septum lysis	Minimal	1 (50)	1 (50)	2	0.55
	Moderate	1 (100)	0 (0)	1	
Cribriform plate lysis	Minimal	1 (33)	2 (67)	3	0.213
	Moderate	1 (100)	0 (0)	1	
Nasal bone or adjacent maxilla lysis	None	3 (33)	6 (67)	9	0.615
	Minimal	2 (40)	3 (60)	5	
	Moderate	2	0 (0)	2	

		(100)			
Frontal sinus soft-tissue attenuation	None Minimal Moderate Severe	1 (33) 1 (100) 4 (80) 1 (14)	2 (67) 0 (0) 1 (20) 6 (86)	3 1 5 7	0.040
Sphenoid sinus soft-tissue attenuation	None Minimal Moderate Severe	4 (57) 0 (0) 1 (100) 2 (29)	3 (43) 1 (100) 0 (0) 5 (71)	7 1 1 7	0.789
Nasopharyngeal soft-tissue attenuation	None Minimal Severe	5 (83) 0 (0) 2 (29)	1 (17) 3 (100) 5 (71)	6 3 7	0.153
Nasopharyngeal mass	No Yes	6 (55) 1 (20)	5 (45) 4 (80)	11 5	0.585
Tympanic bulla involvement	No Yes	5 (36) 2 (100)	9 (64) 0 (0)	14 2	0.175

[a] Variables representing severity were collapsed into two categories–severe and non-severe–for statistical analyses because of limited number of observations in each class

Table 5

Reactive bone lesions of the nasal and paranasal bones on computed tomography in 16 cats with upper respiratory tract aspergillosis

	Categories	SNA Frequency (Row percents)	SOA Frequency (Row percents)	Total	*P*-value[a]
Nasal bone sclerosis	None	2 (22)	7 (77)	9	0.126
	Minimal	3 (60)	2 (40)	5	
	Moderate	2 (100)	0 (0)	2	
Frontal bone sclerosis	None	2 (29)	5 (71)	7	0.541
	Minimal	0 (0)	1 (100)	1	
	Moderate	3 (60)	2 (40)	5	
	Severe	2 (67)	1 (33)	3	
Zygomatic bone sclerosis	None	7 (50)	7 (50)	14	0.475
	Moderate	0 (0)	2 (100)	2	
Cribriform plate sclerosis	None	6 (40)	9 (60)	15	0.438
	Moderate	1 (100)	0 (0)	1	

[a] Variables representing severity were collapsed into two categories–severe and non-severe–for statistical analyses because of limited number of observations in each class

Table 6

Paranasal bone lysis and paranasal soft-tissue abnormalities in 16 cats with upper respiratory tract aspergillosis

	Categories	SNA Frequency (%)	SOA Frequency (%)	Total	*P*-value[a]
Unilateral orbital soft-tissue attenuation	None	7 (100)	0 (0)	7	0.0002
	Severe	0 (0)	8 (100)	8	
Paranasal soft-tissue attenuation (facial)	None	6 (100)	0 (0)	6	0.003
	Mild	0 (0)	1 (100)	1	
	Moderate	1 (100)	0 (0)	1	
	Severe	0 (0)	8 (100)	8	
Paranasal soft-tissue (facial) mass	No	7 (88)	1 (12)	8	0.001
	Yes	0 (0)	8 (100)	8	
Pterygopalatine fossa mass	No	7 (70)	3 (30)	10	0.011
	Yes	0 (0)	6 (100)	6	
Orbital bone lysis	No	3 (100)	0 (0)	3	0.077
	Yes	4 (33)	8 (67)	12	
Orbital bone lysis	None	3 (100)	0 (0)	3	0.231
	Minimal	0 (0)	1 (100)	1	
	Moderate	3 (43)	4 (57)	7	
	Severe	1 (25)	3 (75)	4	
Type of orbital bone lysis	Unilateral	0 (0)	6 (100)	6	0.061
	Bilateral	4 (67)	2 (33)	6	
Frontal bone lysis	None	4 (33)	8 (67)	12	1
	Minimal	2 (100)	0 (0)	2	
	Moderate	1 (50)	1 (50)	2	
Palatine bone lysis	None	4 (33)	8 (67)	12	0.262
	Minimal	2 (100)	0 (0)	2	
	Moderate	0 (0)	1 (100)	1	
	Severe	1 (100)	0 (0)	1	
Zygomatic bone lysis	None	7 (54)	6 (46)	13	0.213

	Minimal	0 (0)	2 (100)	2	
	Moderate	0 (0)	1 (100)	1	
Mandibular lymph node enlargement	Not scanned	0 (0)	1 (100)	1	0.011
	Minimal	4 (100)	0 (0)	4	
	Moderate	3 (50)	3 (50)	6	
	Severe	0 (0)	5 (100)	5	
Retropharyngeal lymph node enlargement	Not scanned	1 (33)	2 (67)	3	0.135
	None	3 (100)	0 (0)	3	
	Minimal	2 (50)	2 (50)	4	
	Moderate	0 (0)	3 (100)	3	
	Severe	1 (33)	2 (67)	3	

[a] Variables representing severity were collapsed into two categories–severe and non-severe–for statistical analyses because of limited number of observations in each class

Figures

Fig. 1. Transverse skull CT images (bone algorithm) of two cats with SNA due to *A. fumigatus* infection showing severe "cavitated" turbinate lysis bilaterally (arrows) (a) and in the left nasal cavity (b).

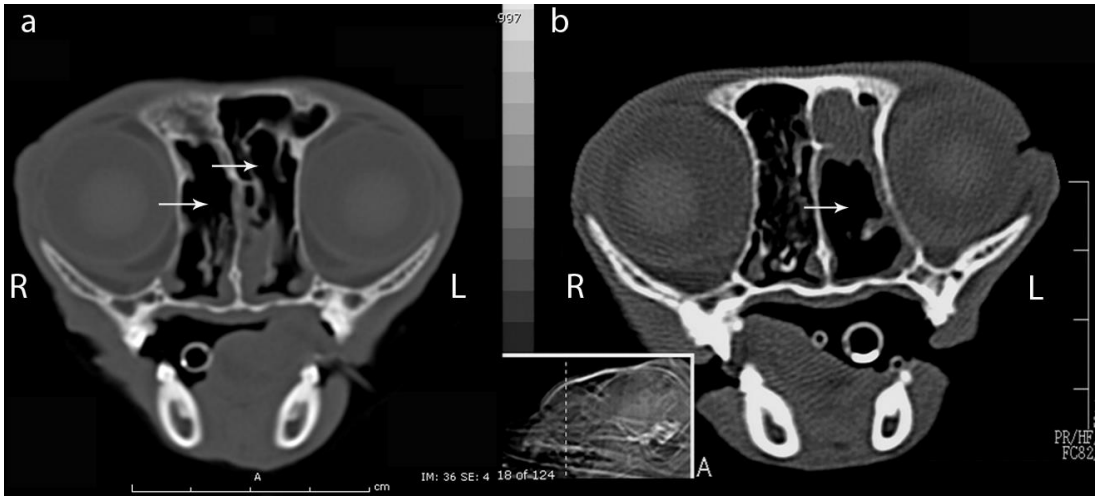

Fig. 2. Transverse skull CT images (bone algorithm) showing right frontal sinus mucosal thickening in a cat with SNA and *A. fumigatus* infection (arrow) (a) and a soft-tissue attenuating mass in the left frontal sinus of a cat with SOA (left orbital mass) due to *A. felis* infection (arrow) (b).

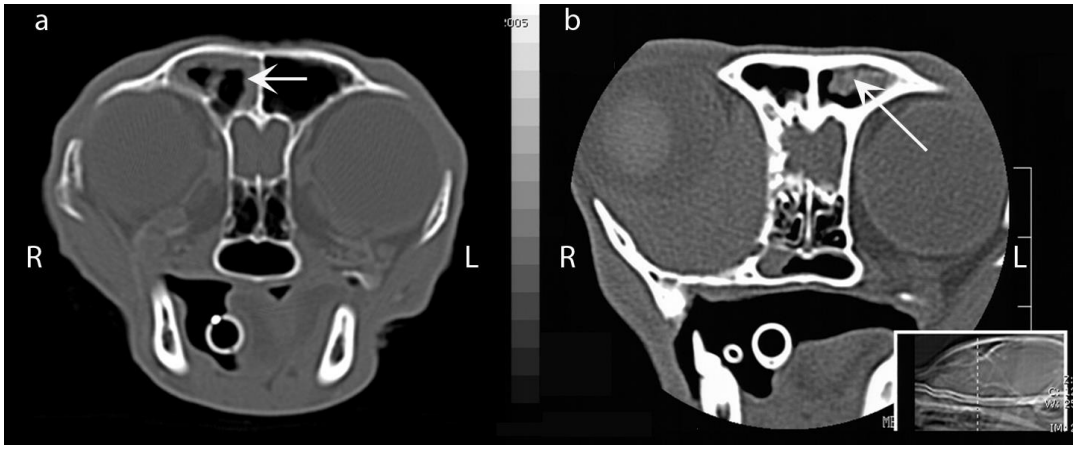

Fig. 3. Dorsal (a) and transverse (b) skull CT images (bone algorithm) showing a calcified density (1835 HU) in the sphenoid sinus of a cat with SOA and *A. udagawae* infection (white arrows). Note the soft-tissue attenuating material in the nasal cavity (a) and frontal sinuses (b) bilaterally (asterisks), and left orbital lysis (black arrow) (a).

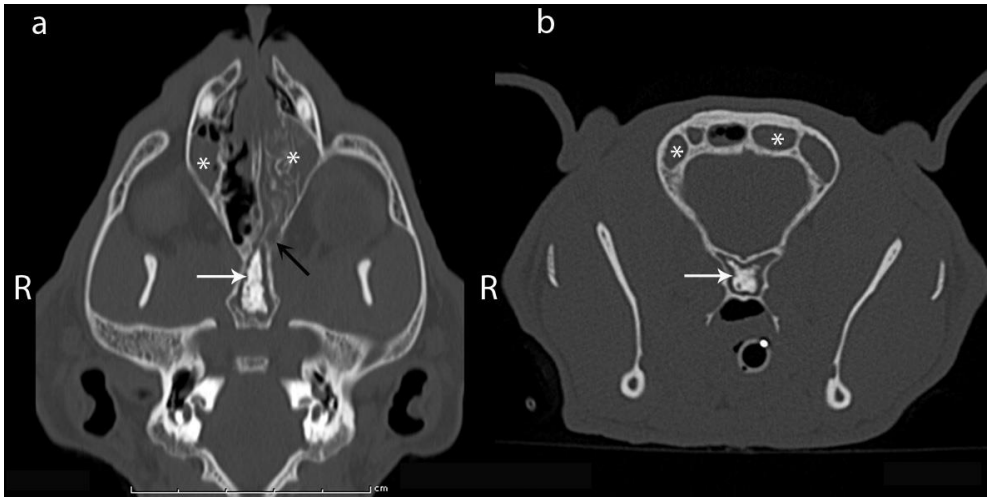

Fig. 4. Transverse post-contrast soft-tissue images of the head reconstructed using a soft-tissue algorithm showing left orbital masses in two cats with SOA and *A. felis* infection. There is heterogeneous contrast enhancement, with central coalescing hypoattenuating foci and peripheral rim enhancement. There is compression (a) and dorsal displacement of the globe (a and b, black arrow), and extension into the oral cavity (a, white arrow), nasopharynx (b, white arrow) and adjacent paranasal maxillary soft-tissues (a and b, black asterisk).

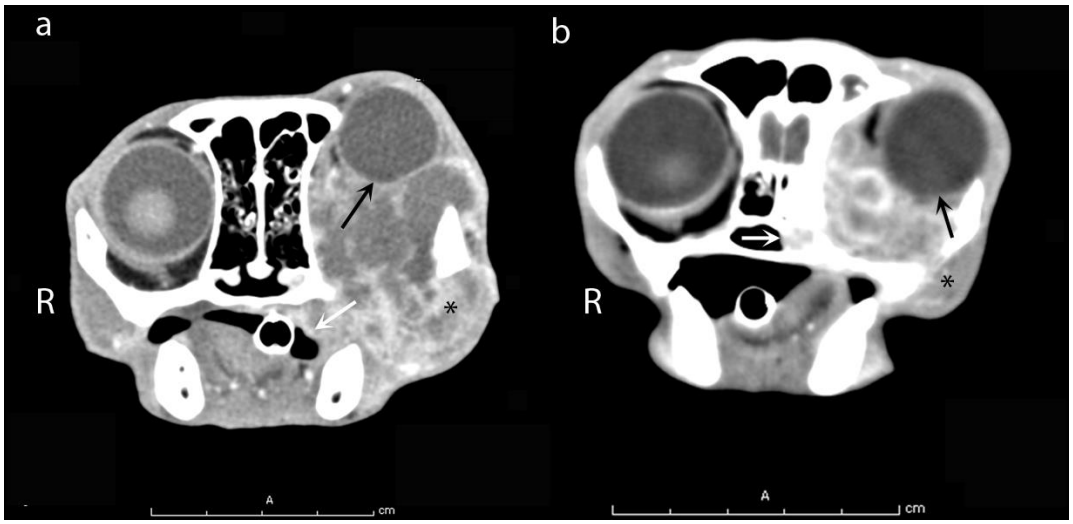

Fig.5. Reconstructed dorsal (a) and transverse (b) skull CTs showing regions of severe complete bilateral orbital lysis (arrow) in a cat with SNA due to *A. felis* (a) and bilateral moderate punctate lysis (arrows) in a cat with SNA due to *A. udagawae* (b).